6316

J. Am. Chem. Soc. **1995,** *117,* 6316–6326

Models for Oxide Interactions in Bimetallic Catalysts: Oxo Clusters by Stepwise Oxidation of a Pt₃Re Cluster

**Jianliang Xiao,[†] Leijun Hao,[†] Richard J. Puddephatt,*,[†]
Ljubica Manojlović-Muir,[‡] and Kenneth W. Muir*,[‡]**

*Contribution from the Departments of Chemistry, University of Western Ontario,
London, Canada N6A 5B7, and University of Glasgow, Glasgow G12 8QQ, Scotland*

Received January 20, 1995[⊛]

Abstract: Oxidation of the complex $[Pt_3\{Re(CO)_3\}(\mu\text{-dppm})_3]^+$ (**1**, dppm = $Ph_2PCH_2PPh_2$) with the oxidants Me_3-NO, PhIO, O_2, or H_2O_2 under mild conditions gives the series of oxo clusters $[Pt_3\{Re(CO)_3\}(\mu_3\text{-O})_n(\mu\text{-dppm})_3]^+$ (**2**, $n = 1$; **3**, $n = 2$; **4**, $n = 3$). In this series, the cluster electron count increases from 54 to 58, 62, and 66 in **1**, **2**, **3**, and **4**, respectively; there is a corresponding decrease in metal–metal bonding in this series and **4** contains no metal–metal bonding. The cluster **3** has been characterized by an X-ray structure determination and the other complexes by spectroscopic methods. Crystals of **3**[PF₆]·OEt₂ are monoclinic, space group $P2_1/n$, $a = 17.1603(18)$ Å, $b = 23.2822(17)$ Å, $c = 19.7021(9)$ Å, $\beta = 94.160(6)°$; $R = 0.047$, $R_w = 0.042$ for 11 822 unique reflections with $I \geq 2\sigma(I)$ and $\theta(\text{Mo K}\alpha) \leq 30°$. The ^{31}P NMR spectra are shown to reflect the extent of Pt–Pt bonding. Oxidation of **4** by H_2O_2 or of **1** or **3** at high temperature by O_2 can also give $[Pt_3(ReO_3)(\mu_3\text{-O})_3(\mu\text{-dppm})_3]^+$ (**5**) and $[Pt_3(ReO_3)(\mu\text{-dppm})_3]^+$ (**6**), respectively, the first examples of a metal–metal bonded cluster containing metals in widely different oxidation states. Cluster **6** is also prepared by reaction of $[Pt_3(\mu_3\text{-H})(\mu\text{-dppm})_3]^+$ with $MeReO_3$. The cluster **3** reacts with donor ligands to give $[Pt_3\{Re(CO)_2L\}(\mu_3\text{-O})_2(\mu\text{-dppm})_3]^+$ (**7**). The nature of the bonding in clusters **1–6** is discussed on the basis of XPS spectra; the oxidation of **1** to **4** causes very little change in the Re $4f_{7/2}$ binding energy but an increase in the Pt $4f_{7/2}$ binding energy whereas there is a large increase in Re $4f_{7/2}$ binding energy on oxidation to **5** and **6**. EHMO calculations indicate that the ReO_3^+ group is a stronger acceptor of electron density from the $Pt_3(\mu\text{-dppm})$ group than is $Re(CO)_3^+$ and support an analogy between the donors $C_5H_5^-$ and $Pt_3(\mu\text{-dppm})_3$. The relevance of these clusters as models of bimetallic $Pt/Re/Al_2O_3$ catalysts is discussed.

Introduction

In developing the analogy between metal clusters and surfaces,[1,2] it is important to recognize that most heterogeneous catalysts are supported on oxide surfaces, often with strong metal-support interactions, and that metal oxides are also used as catalysts.[3] Modeling bimetallic catalysts using cluster complexes presents further challenges and it is not possible to mimic all aspects of a heterogeneous catalyst. In the specific case of the PtRe/Al₂O₃ catalysts which are extensively used in petroleum reforming,[4] there is a consensus that platinum is present at Pt(0) but evidence has been given for rhenium being present as Re(0), Re(II) and Re(IV). The nature of the interaction of either platinum or rhenium with the oxide support

is also uncertain.[5] According to one model, the more oxophilic rhenium may be present, in a positive oxidation state and with ReO bonding present, at the interface between the support and the platinum or Pt–Re alloy particles and so anchor the small catalyst particles to the support.[5] The platinum particles are also known to catalyze the reduction of perrhenate in the formation of the Pt–Re catalysts by hydrogen reduction of adsorbed chloroplatinate and perrhenate salts, and it is possible that clusters containing PtReO units are involved in such reactions.[5] This paper addresses the issue of whether oxo–rhenium–platinum clusters can be prepared and if their chemistry is relevant to the above aspects of the heterogeneous catalyst formation and structure. Metal cluster complexes containing oxo ligands are still relatively uncommon for later transition elements, with most containing only one oxygen atom.[6] There are few general synthetic methods for metal–metal bonded clusters containing oxo ligands, and a large proportion of such clusters have been obtained serendipitously.[7a] This paper reports a detailed study of the oxidation of the complex $[Pt_3\{Re(CO)_3\}(\mu\text{-dppm})_3]^+$ (**1**, dppm = $Ph_2PCH_2PPh_2$).

[†] University of Western Ontario.
[‡] University of Glasgow.
[⊛] Abstract published in *Advance ACS Abstracts,* June 1, 1995.
(1) (a) Mingos, D. M. P.; Wales, D. J. *Introduction to Cluster Chemistry*; Prentice Hall: Englewood Cliffs, NY, 1990. (b) *The Chemistry of Metal Cluster Complexes*; Shriver, D. F., Kaesz, H. D., Adams, R. D., Eds.; VCH: New York, 1990.
(2) Gates, B. C. *Angew. Chem., Int. Ed. Engl.* **1993,** *32,* 228 and references therein.
(3) (a) Gates, B. C. *Catalytic Chemistry*; Wiley: New York, 1992. (b) *Metal-Support Interaction in Catalysis, Sintering, and Redispersion*; Stevenson, S. A., Dumesic, J. A., Baker, R. T. K., Ruckenstein, E., Eds.; Van Nostrand Reinhold: New York, 1987.
(4) (a) Ribeiro, F. H.; Bonivardi, A. L.; Kim, C.; Somorjai, G. A. *J. Catal.* **1994,** *150,* 186. (b) Huang, Z.; Fryer, J. R.; Park, C.; Stirling, D.; Webb, G. *J. Catal.* **1994,** *148,* 478. (c) Borgna, A.; Garetto, T. F.; Monzon, A.; Apesteguia, C. R. *J. Catal.* **1994,** *146,* 69. (d) Biswas, J.; Bickle, G. M.; Gray, P. G.; Do, D. D.; Barbier, J. *Catal. Rev. Sci. Eng.* **1988,** *30,* 161.
(5) (a) Fung, A. S.; McDevitt, M. R.; Tooley, P. A.; Kelley, M. J.; Koningsberger, D. C.; Gates, B. C. *J. Catal.* **1993,** *140,* 190. (b) Hilbrig, F.; Michel, C.; Haller, G. L. *J. Phys. Chem.* **1992,** *96,* 9893. (c) Godbey, D. J.; Somorjai, G. A. *Surf. Sci.* **1988,** *202,* 204. (d) Augustine, S. M.; Sachtler, W. M. H. *J. Catal.* **1989,** *116,* 184. (e) Tysoe, W. T.; Zaera, F.; Somorjai, G. A. *Surf. Sci.* **1988,** *200,* 1.

(6) (a) Ingham, S. L.; Lewis, J.; Raithby, P. R. *J. Chem. Soc., Chem. Commun.* **1993,** 166. (b) Schauer, C. K.; Voss, E. J.; Sabat, M.; Shriver, D. F. *J. Am. Chem. Soc.* **1989,** *111,* 7662. (c) Chi, Y.; Hwang, L. S.; Lee, G. H.; Peng, S. M. *J. Chem. Soc., Chem. Commun.* **1988,** 1456. (d) Gibson, C. P.; Rae, A. D.; Tomchick, D. R.; Dahl, L. F. *J. Organomet. Chem.* **1988,** *340,* C23. (e) Cotton, F. A.; Lahuerta, P.; Sanau, M.; Schwotzer, W. *J. Am. Chem. Soc.* **1985,** *107,* 8284. (f) Schauer, C. K.; Shriver, D. F. *Angew. Chem., Int. Ed. Engl.* **1987,** *26,* 255. (g) Colombie, A.; Bonnet, J.-J.; Fompeyrine, P.; Lavigne, G.; Sunshine, S. *Organometallics* **1986,** *5,* 2305. (h) Goudsmit, R. J.; Johnson, B. F. G.; Lewis, J.; Raithby, P. R.; Whitmire, K. H. *J. Chem. Soc., Chem. Commun.* **1983,** 246. (i) Ceriotti, A.; Resconi, L.; Demartin, F.; Longoni, G.; Manassero, M.; Sansoni, M. *J. Organomet. Chem.* **1983,** *249,* C35. (j) Lavigne, G.; Lugan, N.; Bonnet, J. J. *Nouv. J. Chim.* **1981,** *5,* 423. (k) Bartley, S. L.; Dunbar, K. R.; Shih, K.-Y.; Fanwick, P. E.; Walton, R. A. *J. Chem. Soc., Chem. Commun.* **1993,** 98.

It will be shown that reaction with oxidants Me₃NO, PhIO, O₂, or H₂O₂ under mild conditions can give the series of oxo clusters [Pt₃{Re(CO)₃}(μ_3-O)$_n$(μ-dppm)₃]⁺ (**2**, $n = 1$; **3**, $n = 2$; **4**, $n = 3$) and [Pt₃(ReO₃)(μ_3-O)₃(μ-dppm)₃]⁺ (**5**). In these clusters, the increases in cluster electron count by up to 12 electrons and of the sum of the metal oxidation states by up to 12 units are unprecedented in cluster chemistry. At high temperature, the reaction of cluster **1** with O₂ gives another unusual cluster, [Pt₃-(ReO₃)(μ-dppm)₃]⁺ (**6**). This complex, along with cluster **5**, represents the first examples of a cluster containing metals in widely different oxidation states. A more rational synthesis of **6** and the reactions of **3** with donor ligands are also described. Parts of this work have been described in preliminary communications,[8,9] and it is an extension of studies of the coordinatively unsaturated cluster cation [Pt₃(μ_3-CO)(μ-dppm)₃]²⁺, which acts as a model for chemisorption of small molecules on platinum metal surfaces.[10] Most triangular metal clusters have 48 valence electrons whereas [Pt₃(μ_3-CO)(μ-dppm)₃]²⁺ has only a 42-electron count, and so has three vacant coordination sites, one at each platinum center (the 6p$_z$ orbital in each case).[10] Similarly, most tetrahedral metal clusters have 60 valence electrons whereas cluster **1** has only a 54-electron count and so also has three vacant sites. A similar reactivity as found for [Pt₃(μ_3-CO)(μ-dppm)₃]²⁺ might therefore be expected. However, whereas [Pt₃(μ_3-CO)(μ-dppm)₃]²⁺ adds ligands such as phosphines by coordination to one or more platinum atoms, cluster **1** adds such ligands by coordination to rhenium thus forming [Pt₃{Re(CO)₃L}(μ-dppm)₃]²⁺.[11] The reaction of **1** with oxygen or oxygen atom donors is unique as described below.
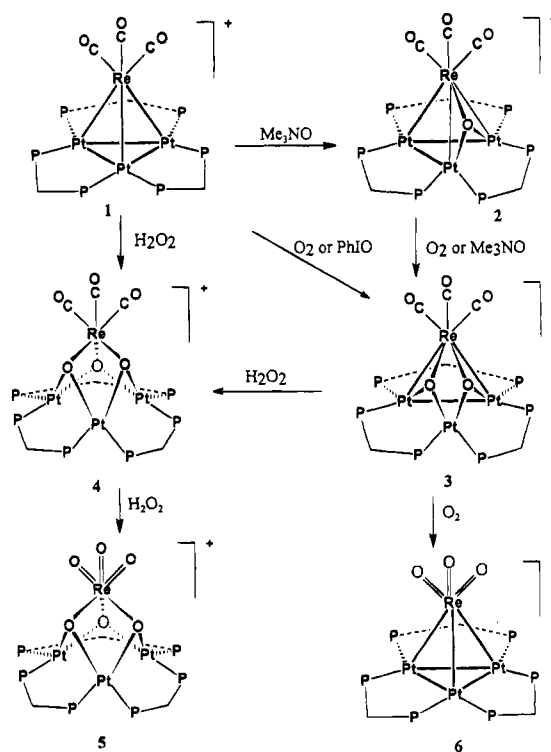
Results

The Oxidation of Cluster Cation 1. A summary of the reactions of cluster cation **1** with oxygen atom donors is shown in Scheme 1.

Black crystals of **1** slowly became orange on exposure to air with formation of the dioxo cluster **3**, and the reaction also occurred slowly (several days) in solution. When the reaction was monitored by NMR, only clusters **1** and **3** were present in detectable amounts and so there are no long-lived intermediates involved. As expected, the reaction is faster under pure O₂ while **1** is stable under a N₂ atmosphere. Hence there is no doubt that O₂ is the oxidant in forming **3** under these conditions.

The reaction of O₂ with **1** to give the dioxo cluster **3** is catalyzed by anions such as OH⁻, Cl⁻, CN⁻, and H⁻. For example, the reaction is about 7 times faster in the presence of KOH than in its absence, and this allows the synthesis of **3** in yields as high as 80% in 1 day. The catalytic effect of anionic nucleophiles such as the halides, CN⁻, and even H⁻ on carbonyl cluster reactions such as ligand substitution has been well documented.[12] The mechanism of these reactions may involve the attack of the nucleophilic anion at the coordinated CO or at the metal with loss of CO, followed by ligand coordination. Typical examples are seen in the anion-catalyzed reactions of

(7) (a) Bottomley, F.; Sutin, L. *Adv. Organomet. Chem.* **1988**, *28*, 339. (b) Nugent, W. A.; Mayer, J. M. *Metal-Ligand Multiple Bonds*; Wiley: New York, 1988.

(8) Xiao, J.; Vittal, J. J.; Puddephatt, R. J.; Manojlović-Muir, L.; Muir, K. W. *J. Am. Chem. Soc.* **1993**, *115*, 7882.

(9) Xiao, J.; Puddephatt, R. J.; Manojlović-Muir, L.; Muir, K. W.; Torali, A. A. *J. Am. Chem. Soc.* **1994**, *116*, 1129.

(10) Puddephatt, R. J.; Manojlović-Muir, Lj.; Muir, K. W. *Polyhedron* **1990**, *9*, 2767.

(11) Xiao, J.; Hao, L.; Puddephatt, R. J.; Manojlović-Muir, L.; Muir, K. W.; Torabi, A. A. *Organometallics* In Press.

(12) Lavigne, G. In *The Chemistry of Metal Cluster Complexes*; Shriver, D. F., Kaesz, H. D., Adams, R. D., Eds.; VCH: New York, 1990.

Scheme 1

[Ru₃(CO)₁₂], which may lead to substitution of CO by phosphines or ¹³CO or to reaction with H₂, with rates that are orders of magnitude faster than without the anions.[12] The present reaction is different since no CO dissociation takes place. Earlier study showed that there exists an equilibrium between complex **1** and the halide ions (eq 1,X = Cl, Br, or I), with the

$$(1)$$
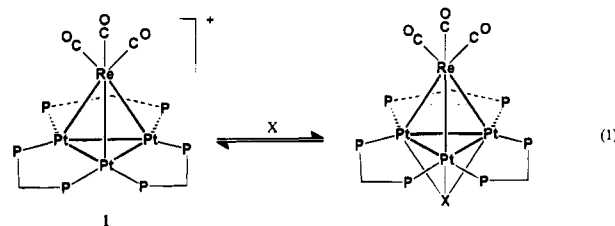
halide adduct being favored in the order I⁻ > Br⁻ > Cl⁻.[13] No such adducts have been detected with OH⁻, H⁻, or CN⁻, but reversible coordination to **1**, with a lower equilibrium constant, is possible. Although CO is not displaced in the present case, coordination of the anions to the Pt₃ face may be expected to weaken the PtRe bonding, as evidenced by the structural determination of the iodo adduct.[11] Therefore, one possible explanation for the observed rate acceleration is that the anion coordination weakens the PtRe bonding and so facilitates access of O₂ between the platinum and rhenium centers.

A better route to the dioxo cluster **3** is provided by reaction of **1** with oxygen donors, Me₃NO and PhIO. The yields were high and the reactivity followed the sequence PhIO > Me₃NO > O₂. Interestingly, the reaction involving Me₃NO proceeded via an intermediate species, identified as the monooxo cluster [Pt₃{Re(CO)₃}(μ_3-O)(μ-dppm)₃]⁺ (**2**). Complex **2** was formed within 1 h of the addition of the oxygen donor while its further transformation to the dioxo cluster **3** took several hours to completion. If only 1 equiv of Me₃NO was used, **2** was the major product, but some **1** and **3** were also present. The

(13) Xiao, J.; Hao, L.; Puddephatt, R. J.; Manojlović-Muir, L.; Muir, K. W.; Torabi, A. A. *J. Chem. Soc., Chem. Commun.* **1994**, 2221.

identification of **2** is therefore based on spectroscopic and reactivity studies only. Complex **2** is stable under a nitrogen atmosphere but it is oxidized in air over a period of about 1 day to give **3**. The monooxo cluster could not be detected in the reaction of **1** with O_2 to give **3**, and so it is not an intermediate in this reaction. A separate study shows that **1** reacts somewhat more slowly with O_2 than does **2**, but the difference is not great and so **2** would be expected to be detectable at intermediate stages of the oxidation of **1** with O_2 if it were formed. Neither the oxygen donors nor O_2 were capable of further oxidation of **3** under mild conditions.

The trioxo cluster **4** was readily prepared in high yield by treatment of complex **1** with H_2O_2. The reaction was characterized by a dramatic color change from deep red-black to yellow. By monitoring the reaction by NMR, it was shown that complex **3** was formed immediately after mixing **1** with hydrogen peroxide while the transformation of **3** to **4** via reaction with more H_2O_2 took several hours to reach completion. The cluster **4** could also be generated in good yield by irradiation of a solution of **1** in tetrahydrofuran in the presence of oxygen, a reaction which also involves the intermediacy of **3**. Accordingly, treatment of **3** with H_2O_2 afforded **4** in high yield. The novel hexaoxo cluster **5** was obtained by further oxidation of **4** with H_2O_2. The reaction takes several hours to reach completion. Complex **5** is white in color and has low solubility in acetone and CH_2Cl_2. The formation of these polyoxo clusters with hydrogen peroxide appears to be unprecedented in cluster chemistry, and may provide a path to other unusual oxo clusters.

The remarkable terminal trioxo cluster $[Pt_3(ReO_3)(\mu\text{-dppm})_3]^+$ (**6**) was first prepared by the reaction of **1** with O_2 in refluxing *o*-xylene. By monitoring the reaction by NMR, it was shown that the initial product was the dioxo cluster **3**, but more extended reflux resulted in further oxidation to give **6[PF$_6$]**, which decomposed slowly with formation of **6[ReO$_4$]**. The $[ReO_4]^-$ ion is clearly formed by further oxidation of the Pt_3-(ReO_3) group in **6**. The oxidation of Re–CO groups to Re=O groups on going from **1** to **5** and **6** finds precedent in the oxidation of $[(\eta^5\text{-}C_5Me_5)Re(CO)_3]$, which may be considered isolobal to cluster **1** (see below), to $[(\eta^5\text{-}C_5Me_5)ReO_3]$ by using H_2O_2 or $O_2/h\nu$.[14] However, there is a significant mechanistic difference between the oxidations of **1** and $[(\eta^5\text{-}C_5Me_5)Re(CO)_3]$: for the metal cluster, oxidation by oxygen atom addition evidently takes place first at the Pt–Re bonds, and the $Re(CO)_3$ to $Re(=O)_3$ transformation has a higher activation energy.

An attractive mechanism for formation of **6** would be oxidation of **3** to **4** followed by dissociation of the carbonyl ligands from rhenium and effective inversion of the ReO_3 unit, thus converting the $Pt_3Re(\mu_3\text{-O})_3$ group to $Pt_3Re(=O)_3$, but this route is not supported by the evidence. Thus, cluster **4** was not detected at intermediate stages of the reaction leading to **6** and attempts to convert the trioxo cluster **4** to **6** have not been successful. For example, when a solution of **4** in *o*-xylene was heated under reflux, a complex mixture of decomposition products was formed but no **6** was detected at any stage as monitored by NMR. The mechanism of formation of **6** by oxidation of **1** by O_2 in refluxing xylene is therefore not yet understood. The key step is clearly the conversion of **3** to **6**, apparently without the intermediacy of **4**. The rate of this reaction is not reproducible in our hands, and there is a clear induction period before reaction begins. It is possible that one of the decomposition products acts as a catalyst for the reaction.

Whatever the cause, the lack of reproducibility is a problem in synthesis since each reaction must be monitored carefully by NMR.

Although complex **6[PF$_6$]** may be obtained in yields as high as 90% by the above method, some attempted syntheses were much less successful and so a more reliable route was sought. It has now been found that the trioxo cluster **6[PF$_6$]** can be obtained readily and reproducibly in high yield (80%) by treatment of $[Pt_3(\mu_3\text{-H})(\mu\text{-dppm})_3]^+$ with $[MeReO_3]$ (eq 2).[15,16]

$$(2)$$
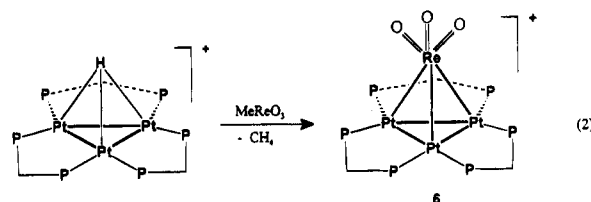
The reaction was complete within a few seconds at room temperature and was accompanied by evolution of methane. Since both starting complexes are easily accessible, this method provides a far better entry to the trioxo cluster **6** than the previous one. In addition, it is possible that the reaction of a cluster containing the $M_3(\mu_3\text{-H})$ group with $MeReO_3$ may provide a more general method for synthesis of the $M_3(\mu_3\text{-ReO}_3)$ group.

Reactivity of 3 and Synthesis of $[Pt_3\{Re(CO)_2L\}(\mu\text{-O})_2\text{-}(\mu\text{-dppm})_3]^+$ (7). The coordinatively unsaturated cluster **1** reacts rapidly with ligands by addition to the rhenium center.[11] In contrast, the more electron-rich cluster complex **3** reacts slowly with some ligands by substitution of a carbonyl ligand at the rhenium center. For example, **3** reacted with $P(OMe)_3$ to give the new dioxo species **7a** (eq 3), and the reaction took

$$(3)$$

$$L = P(OMe)_3, \mathbf{7a}; P(OPh)_3, \mathbf{7b}$$
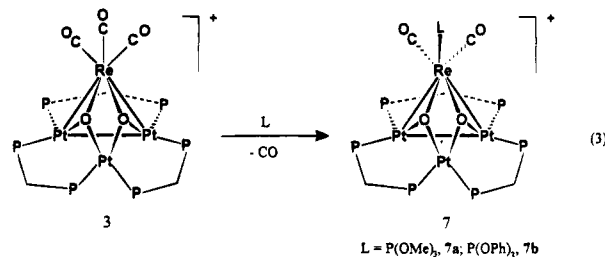
over 20 h to complete. This reaction resembles the reaction of $[\eta^5\text{-CpRe(CO)}_3]$ with neutral ligands under UV irradiation, where CO substitution instead of ligand addition usually takes place.[17] The oxo cluster $[Os_6(\mu_3\text{-O})(\mu_3\text{-CO})(CO)_{18}]$ reacts with excess $P(OMe)_3$ in refluxing benzene, by addition of the phosphite but with loss of the capping oxo ligand instead of a carbonyl ligand.[6h]

The reaction of **3** with ^{13}CO leads to the exchange of the CO ligands of **3**, and no intermediate species such as a tetracarbonyl adduct was detected during the course of the reaction. ^{13}C NMR monitoring showed that the resonance due to the coordination ^{13}CO in **3** increased slowly with time, so the reaction may proceed in a stepwise manner, leading first to a monosubstituted species analogous to **7** but with $L = {}^{13}CO$, which reacts further with ^{13}CO to give the final product, $[Pt_3\{Re(^{13}CO)_3\}(\mu_3\text{-O})_2\text{-}(\mu\text{-dppm})_3]^+$.

Characterization of the Cluster Cations. The structure of cation **3**, shown in Figure 1, was established by an X-ray

(14) (a) Herrmann, W. A.; Serrano, R.; Bock, H. *Angew. Chem., Int. Ed. Engl.* **1984**, *23*, 383. (b) Herrmann, W. A. *Angew. Chem., Int. Ed. Engl.* **1988**, *27*, 1297.

(15) Lloyd, B. R.; Puddephatt, R. J. *J. Am. Chem. Soc.* **1985**, *107*, 7785.

(16) Herrmann, W. A.; Kuchler, J. G.; Felixberger, J. K.; Herdtweck, E.; Wagner, W. *Angew. Chem., Int. Ed. Engl.* **1988**, *27*, 394.

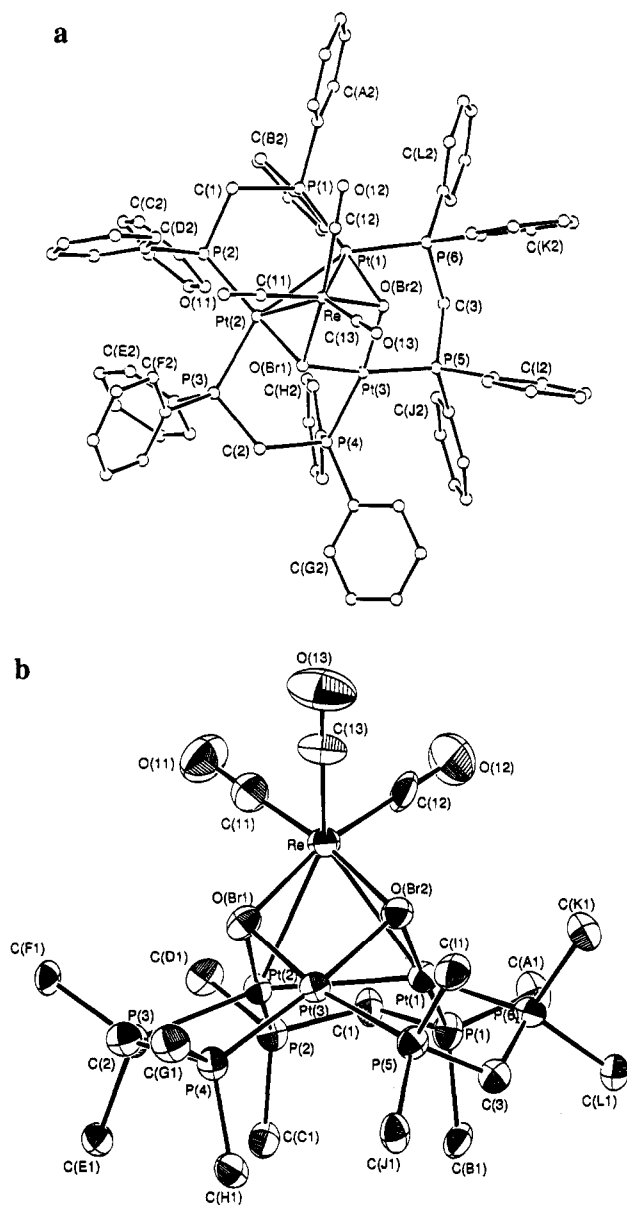(17) Choi, M.-G.; Angelici, R. J. *J. Am. Chem. Soc.* **1991**, *113*, 5651.

a

b

Figure 1. (a) The structure of **3**. The phenyl carbon atoms are numbered in sequence C(n1)$\cdots$C(n6) (n = A, L), starting with the P-substituted atom. Ring labels are placed adjacent to C(n2). Atoms are represented by spheres of arbitrary size. All H-atoms are omitted for clarity. (b) A view of the inner core of **3**, showing 50% probability. Only the ipso carbon atoms of the dppm phenyl groups are shown.

crystallographic study of the salt **3**[PF$_6$] $\cdot$ OEt$_2$. Selected bond lengths and angles are given in Table 1.

The structure of **3** contains a distorted tetrahedral arrangement of metal atoms with each edge of the Pt$_3$ triangle bridged by a dppm ligand, and with two Pt$_2$Re triangles capped by triply bridging oxygen atoms. The Pt$_3$Re(CO)$_3$P$_6$ skeleton approximates to C_s symmetry, the mirror plane passing through the Re and the Pt(3) atoms and bisecting the Pt(1)$-$Pt(2) bond.

Addition of two μ_3-oxo ligands to **1** causes a substantial disruption of the metal$-$metal bonding, which is evident from the highly significant lengthening of all M$-$M distances. In **3** the Pt(1)$-$Pt(2) distance [2.826(1) Å] is more than 0.2 Å longer, and the Pt(1)$-$Re and Pt(2)$-$Re distances [2.843(1) and 2.854-(1) Å] are more that 0.15 Å longer, than the corresponding distances in **1**; nevertheless, they still remain in the accepted ranges of Pt$-$Pt (2.6$-$2.8 Å) and Pt$-$Re (2.7$-$2.9 Å) single bond distances.[18] The Pt(3)$-$Pt(1) and Pt(3)$-$Pt(2) distances [3.094(1) and 3.081(1) Å] are even longer and are outside the

normal range of Pt$-$Pt covalent bond distances. They are on the borderline of weak bonding interactions and nonbonding contacts: a Pt$-$Pt distance as long as 3.07 Å has been regarded as evidence of weak metal$-$metal bonding but is best regarded as nonbonding in the present case.[19] The Pt(3)$-$Re distance [3.228(1) Å] is clearly a nonbonding contact. Thus in **3** the metal atoms are held by normal covalent bonds in the Pt(1)Pt-(2)Re triangle only, whereas in **1** they are held by six bonds coinciding with all edges of the Pt$_3$Re tetrahedron [Pt$-$Pt 2.593-(1)$-$2.611(1) Å and Pt$-$Re 2.649(1)$-$2.685(1) Å]. Assuming that a μ_3-O ligand is a 4-electron donor, the electron count increases from 54 in **1** to 62 in **3**, and therefore lengthening and even cleavage of the M$-$M bonds in **3** is expected. In contrast, incorporation of μ_3-O ligands in clusters in which the electron count remains the same causes shortening of M$-$M bonds.[6i,j]

In **3** the μ_3-oxo ligands bind to the Pt$_2$Re triangles in nearly symmetrical fashion. The Pt$-$O bonds [2.036(6)$-$2.065(6) Å] are slightly shorter than the Re$-$O bonds [2.117(6) and 2.121-(6) Å], but both are in agreement with bond lengths observed in other complexes.[6] Thus, for example, in different solvates of [Pt$_4$(μ_3-O)$_2$Cl$_2$(dmso)$_6$] (dmso = dimethyl sulfoxide), the mean Pt^{II}$-$O and Pt^I$-$O distances are 2.03 and 2.06 Å while, in the salts of the [Re$_3$(μ_3-O)(μ-H)$_3$(CO)$_9$]$^{2-}$ anion, the mean Re$-$O distances are 2.12$-$2.13 Å.[20] The μ_3-bridging is the most common bonding mode of oxygen atoms in metal clusters,[6] and it is also common on metal surfaces.[21] However, it has been noted that clusters containing two μ_3-O ligands are rare for the late transition metals.[7a] Examples of M$_3$(μ_3-O) groups are found in [Ir$_3$(μ_3-O)$_2$(μ_2-I)(COD)$_3$], where COD = 1,5-cyclooctadiene[6e] and [Pt$_4$(μ_3-O)$_2$Cl$_2$(dmso)$_6$].[20a]

The latitudinal Pt$_3$P$_6$ skeleton in the Pt$_3$(μ-dppm)$_3$ fragment is approximately planar in [Pt$_3$(μ_3-CO)(μ-dppm)$_3$]$^{2+}$,[10] whereas in **3** it is severely distorted. The Pt$-$P bonds are bent out of the Pt$_3$ plane and away from the μ_3-oxo bridges (Figure 1b), the out-of-plane displacements of the P atoms ranging from 0.68 to 1.11 Å. The Pt$-$P bond lengths fall into two groups: the four bonds roughly *trans* to μ_3-O atoms [2.227(3)$-$2.243(3) Å] are shorter than the other two [2.306(3) and 2.318(3) Å].

The spectroscopic data for **3** are fully consistent with the structure revealed by X-ray diffraction. The IR spectrum displayed three terminal carbonyl stretches ranging from 1852 to 1974 cm^{-1}. The frequencies of these bands are somewhat *lower* than those found for **1** (1979, 1873, and 1867 cm^{-1}); this is counter-intuitive since the conversion of cluster **1** to **3** is clearly an oxidation and might be expected to lead to an increase in ν(CO) values. The ^{31}P NMR spectrum of **3** showed three resonances (Figure 2), as is expected from the structure in Figure 1 which, in idealized form, contains a plane of symmetry. A closer analysis of the spectrum gives further insight into the structure of **3**. The spectrum can be analyzed in terms of an (AMX)$_2$ spin system due to coupling between nonequivalent phosphorus atoms P^a, P^b, and P^c as shown, with the satellites due to $J(^{195}$Pt^{31}P) couplings. The multiplet at δ 5.3 can be assigned to P^b, which is expected to couple to both P^a and P^c.

(18) (a) Douglas, G.; Manojlović-Muir, Lj.; Muir, K. W.; Rashidi, M.; Anderson, C. M.; Puddephatt, R. J. *J. Am. Chem. Soc.* **1987**, *109*, 6527 and references therein. (b) Ciani, G.; Moret, M.; Sironi, A.; Antognazza, P.; Beringhelli, T.; D'Alfonso, G.; Pergola, R. D.; Minoja, A. *J. Chem. Soc., Chem. Commun.* **1991**, 1255. The Cambridge Structure Database yielded references to 15 structures containing Pt$-$R bonds.

(19) Ciani, G.; Moret, M.; Sironi, A.; Beringhelli, T.; D'Alfonso, G.; Pergola, R. D. *J. Chem. Soc., Chem. Commun.* **1990**, 1668.

(20) (a) Betz, P.; Bino, A. *J. Am. Chem. Soc.* **1988**, *110*, 602. (b) Beringhelli, T.; D'Alfonso, G.; Feni, M.; Ciani, G.; Molinari, H. *J. Organomet. Chem.* **1986**, *311*, 177 and references therein.

(21) Somorjai, G. A. *Chemistry in Two Dimensions: Surfaces*; Cornell University Press: New York, 1981.

Table 1. Selected Interatomic Distances (Å) and Angles (deg) in Complex **3**

Pt(1)−Pt(2)	2.826(1)	Pt(1)···Pt(3)	3.094(1)	Pt(1)−Re	2.843(1)	Pt(1)−P(1)	2.227(3)
Pt(1)−P(6)	2.306(3)	Pt(1)−O(Br2)	2.049(6)	Pt(2)···Pt(3)	3.081(1)	Pt(2)−Re	2.854(1)
Pt(2)−P(2)	2.227(3)	Pt(2)−P(3)	2.318(3)	Pt(2)−O(Br1)	2.065(6)	Pt(3)···Re	3.228(1)
Pt(3)−P(4)	2.232(3)	Pt(3)−P(5)	2.243(3)	Pt(3)−O(Br1)	2.036(6)	Pt(3)−O(Br2)	2.046(6)
Re−O(Br1)	2.117(6)	Re−O(Br2)	2.121(6)	Re−C(11)	1.893(11)	Re−C(12)	1.887(10)
Re−C(13)	1.888(10)						

Pt(2)−Pt(1)−Pt(3)	62.5(1)	Pt(2)−Pt(1)−Re	60.5(1)	Pt(2)−Pt(1)−P(1)	91.2(1)
Pt(2)−Pt(1)−P(6)	147.3(1)	Pt(2)−Pt(1)−O(Br2)	87.3(2)	Pt(3)−Pt(1)−Re	65.7(1)
Pt(3)−Pt(1)−P(1)	143.9(1)	Pt(3)−Pt(1)−P(6)	89.7(1)	Pt(3)−Pt(1)−O(Br2)	40.9(2)
Re−Pt(1)−P(1)	124.3(1)	Re−Pt(1)−P(6)	125.8(1)	Re−Pt(1)−O(Br2)	48.1(2)
P(1)−Pt(1)−P(6)	104.3(1)	P(1)−Pt(1)−O(Br2)	171.5(2)	P(6)−Pt(1)−O(Br2)	81.2(2)
Pt(1)−Pt(2)−Pt(3)	63.01(1)	Pt(1)−Pt(2)−Re	60.1(1)	Pt(1)−Pt(2)−P(2)	93.4(1)
Pt(1)−Pt(2)−P(3)	149.7(1)	Pt(1)−Pt(2)−O(Br1)	87.1(2)	Pt(3)−Pt(2)−Re	65.8(1)
Pt(3)−Pt(2)−P(2)	149.3(1)	Pt(3)−Pt(2)−P(3)	91.5(1)	Pt(3)−Pt(2)−O(Br1)	41.0(2)
Re−Pt(2)−P(2)	121.3(1)	Re−Pt(2)−P(3)	126.4(1)	Re−Pt(2)−O(Br1)	47.7(2)
P(2)−Pt(2)−P(3)	103.2(1)	P(2)−Pt(2)−O(Br1)	166.0(2)	P(3)−Pt(2)−O(Br1)	82.7(2)
Pt(1)−Pt(3)−Pt(2)	54.5(1)	Pt(1)−Pt(3)−Re	53.4(1)	Pt(1)−Pt(3)−P(4)	135.0(1)
Pt(1)−Pt(3)−P(5)	92.3(1)	Pt(1)−Pt(3)−O(Br1)	80.6(2)	Pt(1)−Pt(3)−O(Br2)	40.9(2)
Pt(2)−Pt(3)−Re	53.7(1)	Pt(2)−Pt(3)−P(4)	90.2(1)	Pt(2)−Pt(3)−P(5)	138.3(1)
Pt(2)−Pt(3)−O(Br1)	41.7(2)	Pt(2)−Pt(3)−O(Br2)	80.7(2)	Re−Pt(3)−P(4)	130.0(1)
Re−Pt(3)−P(5)	129.1(1)	Re−Pt(3)−O(Br1)	39.9(2)	Re−Pt(3)−O(Br2)	40.1(2)
P(4)−Pt(3)−P(5)	100.9(1)	P(4)−Pt(3)−O(Br1)	90.2(2)	P(4)−Pt(3)−O(Br2)	169.8(2)
P(5)−Pt(3)−O(Br1)	168.9(2)	P(5)−Pt(3)−O(Br2)	89.0(2)	O(Br1)−Pt(3)−O(Br2)	80.0(3)
Pt(1)−Re−Pt(2)	59.5(1)	Pt(1)−Re−Pt(3)	60.9(1)	Pt(1)−Re−O(Br1)	85.7(2)
Pt(1)−Re−O(Br2)	46.0(2)	Pt(1)−Re−C(11)	130.6(3)	Pt(1)−Re−C(12)	82.5(3)
Pt(1)−Re−C(13)	138.6(4)	Pt(2)−Re−Pt(3)	60.5(1)	Pt(2)−Re−O(Br1)	46.2(2)
Pt(2)−Re−O(Br2)	85.2(2)	Pt(2)−Re−C(11)	86.8(3)	Pt(2)−Re−C(12)	121.1(4)
Pt(2)−Re−C(13)	151.5(4)	Pt(3)−Re−O(Br1)	38.1(2)	Pt(3)−Re−O(Br2)	38.4(2)
Pt(3)−Re−C(11)	134.0(3)	Pt(3)−Re−C(12)	136.7(3)	Pt(3)−Re−C(13)	105.3(3)
O(Br1)−Re−O(Br2)	76.5(3)	O(Br1)−Re−C(11)	96.0(4)	O(Br1)−Re−C(12)	166.5(4)
O(Br1)−Re−C(13)	106.7(4)	O(Br2)−Re−C(11)	171.5(4)	O(Br2)−Re−C(12)	99.6(4)
O(Br2)−Re−C(13)	97.6(4)	C(11)−Re−C(12)	86.8(5)	C(11)−Re−C(13)	88.2(5)
C(12)−Re−C(13)	86.5(5)	Pt(1)−P(1)−C(1)	111.2(3)	Pt(2)−P(2)−C(1)	111.7(3)
Pt(2)−P(3)−C(2)	109.9(3)	Pt(3)−P(4)−C(2)	109.5(3)	Pt(3)−P(5)−C(3)	111.6(3)
Pt(1)−P(6)−C(3)	108.5(3)	Pt(2)−O(Br1)−Pt(3)	97.4(3)	Pt(2)−O(Br1)−Re	86.1(3)
Pt(3)−O(Br1)−Re	102.0(3)	Pt(1)−O(Br2)−Pt(3)	98.2(3)	Pt(1)−O(Br2)−Re	86.0(3)
Pt(3)−O(Br2)−Re	101.5(3)	P(1)−C(1)−P(2)	110.6(5)	P(3)−C(2)−P(4)	120.5(5)
P(5)−C(3)−P(6)	120.4(5)	Re−C(11)−O(11)	176.4(9)	Re−C(12)−O(12)	179.2(11)
Re−C(13)−O(13)	176.9(9)				
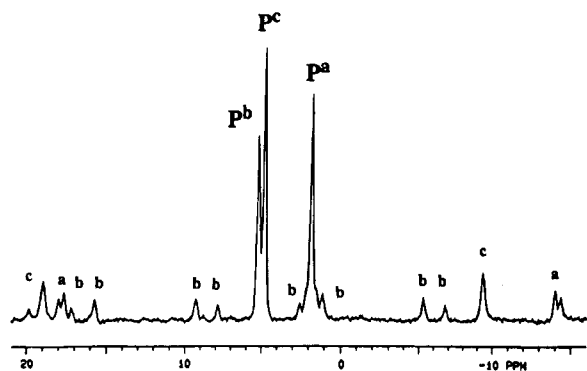
Figure 2. The ^{31}P NMR spectrum of complex **3**.

Further support for the assignment stems from the observation of long-range couplings $^2J(\text{Pt}^1\text{P}^b)$ and $^3J(\text{P}^b\text{P}^b)$, which are commonly observed only for approximately linear P−Pt−Pt−P units containing a metal−metal bond.[22] The corresponding long-range couplings $^2J(\text{PtP})$ and $^3J(\text{P}^a\text{P}^c)$ are not observed in the multiplets assigned to P^a and P^c, indicating that there is no Pt−Pt bond connecting P^a and P^c. The coupling $^2J(\text{P}^a\text{P}^a)$ is observed in the ^{195}Pt satellites of the P^a resonance. The spectrum therefore supports the conclusion from the structure determination, in terms of the distribution of Pt−Pt bonds in **3**. The magnitude of $^1J(\text{PtP}^b) = 2733$ Hz is typical for a phosphorus *trans* to a Pt−Pt bond and is smaller than $^1J(\text{PtP}^a) = 3887$ Hz

and $^1J(\text{PtP}^c) = 3440$ Hz in which phosphorus is *trans* to oxygen. Thus, these couplings correlate with the Pt−P bond distances, the shorter Pt−P distances giving rise to higher $^1J(\text{PtP})$ values.

The IR spectrum of **7a** contained two carbonyl bands at 1894 and 1805 cm^{-1}. The observation of only two carbonyl bands with lower values of $\nu(\text{CO})$ than in **3** is fully consistent with the proposed structure. The ^{31}P NMR spectrum of the complex showed three resonances due to the dppm phosphorus atoms with very similar parameters as in **3**. The phosphite ligand appeared at δ 135, which may be interpreted as a 1:8:18:8:1 quintet due to coupling to two equivalent platinum atoms with $^2J(\text{PtP}) = 82$ Hz. In the structure of **7**, two of the Pt atoms can give couplings $^2J(\text{PtReP})$ through the PtRe bonds, whereas the third platinum would need to give a coupling $^3J(\text{PtOReP})$, and this is presumably too small to be resolved. This supports the interpretation that there are only two Pt−Re bonds. The spectroscopic parameters of **7b** closely resemble those found for **7a**.

The reaction of **3** with ^{13}CO yields [Pt$_3$\{Re(^{13}CO)$_3$\}(μ_3-O)$_2$-(μ-dppm)$_3$]$^+$. The ^{13}C NMR spectrum of this complex contained a singlet due to the coordinated ^{13}CO, at δ 201.2 and room temperature. However, at −90 °C this resonance split to give two singlets with 2:1 intensity, indicating that rotation of the Re(CO)$_3$ group is frozen out at low temperature.

The IR spectrum of cluster **2** contained two CO stretches with frequencies between those of **1** and **3**, at 1978 and 1864 cm^{-1}. The ^{31}P NMR spectrum of **2** contained three resonances indicating that there is 2-fold symmetry. However, the spectrum is more complicated than for **3** due to the couplings between

(22) (a) Rashidi, M.; Puddephatt, R. J. *J. Am. Chem. Soc.* **1986**, *108*, 7111. (b) Ling, S. S. M.; Hadj-Bagheri, N.; Manojlović-Muir, Lj.; Muir, K. W.; Puddephatt, R. J. *Inorg. Chem.* **1987**, *26*, 231.

the three nonequivalent phosphorus atoms. The high-field multiplet assignable to P^b contained satellites with ^1J(PtP) = 4172 Hz due to phosphorus *trans* to oxygen. As with the case of **3**, no long-range couplings were revealed for this phosphorus, indicating that there is no Pt—Pt bond between the two P^b atoms. The low-field multiplets may be analyzed as an [AB]$_2$ multiplet due to P^a and P^c with a coupling ^3J(P^{a}P^c) = 187 Hz and with satellites due to the couplings ^1J(PtP^a) = 2430 Hz and ^1J(PtP^c) = 2600 Hz, indicating that these phosphorus atoms are *trans* to Pt—Pt bonds. Together with the long-range coupling between P^a and P^c, this indicates that there are two Pt—Pt bonds in **2** as proposed.

Although crystals of **4** could be obtained easily, they were not of X-ray quality, so the complex was characterized spectroscopically. The IR spectrum contained two terminal CO bands at 1987 and 1856 cm^{-1}. The similar appearance of these ν(CO) bands to those in **2** and **3** is a clear indication that the Re(CO)$_3$ fragment remains intact during oxidation with H$_2$O$_2$. The ^{31}P NMR spectrum of the cluster contained a singlet due to the dppm ligands, indicating 3-fold symmetry. The coupling constant ^1J(PtP) = 3401 Hz is in the range found for phosphorus *trans* to oxygen, and no long-range couplings ^3J(PP) and ^2J(PtP) characteristic of the M—M bonded Pt$_3$(dppm)$_3$ triangle were observed,[22] indicating that all three Pt—Pt bonds in **1** have been broken during the oxidation to give **4**. The evidence from the ^{31}P NMR spectra therefore indicates that **1**, **2**, **3**, and **4** have 3, 2, 1, and 0 Pt—Pt bonds, respectively, as the electron count of the cluster increases from 54, 58, 62, and 66, respectively.

Complex **5** was also characterized spectroscopically. The XPS analysis is consistent with the complex having a Pt/Re/O atomic ratio of 3/1/6. The IR spectrum of **5** displayed no bands due to ν(CO) but contained bands due to ν(Re=O) at 937 and 900 cm^{-1}, comparable to those observed in **6** (see below) and [(η^5-C$_5$Me$_5$)ReO$_3$] (909 and 878 cm^{-1}).[14] Complex **5** gave a single resonance in the ^{31}P NMR spectrum due to the phosphorus atoms and two resonances in the ^{1}H NMR spectrum due to the CH$_2$P$_2$ protons of the dppm ligands, indicating C_{3v} symmetry. The magnitude of the coupling ^1J(PtP) (3561 Hz) is similar to that observed for **4**, and no long-range couplings J(PtP) were observed, indicating that there are no Pt—Pt bonds in the complex. Since a terminal oxo ligand donates 2 electrons, the electron count of **5** is the same as that of **4** at 66 electrons, so Pt—Pt bonds are not expected. We know of no cluster complexes containing the type of rhenium coordination found in **5**, but related mononuclear complexes are known.[23] For example, the complex [LReO$_3$]$^+$ (L = 1,4,7-triazacyclononane, 1,4,7-trithiacyclononane) is related to **5** if the Pt$_3$O$_3$ ring is considered as a tridentate pseudo crown ether ligand.[23]

The IR spectrum of [Pt$_3$(ReO$_3$)(μ-dppm)$_3$]$^+$ (**6**) gave two bands owing to ν(Re=O) in the Re(=O)$_3$ fragment at 935 and 890 cm^{-1} in **6**[ReO$_4$] and at 925 and 893 cm^{-1} in **6**[PF$_6$]. In addition, the spectrum of **6**[ReO$_4$] contained two bands at 915 and 905 cm^{-1} which are assigned to ν(Re=O) of ReO$_4^-$, based on comparison with **6**[PF$_6$] which does not contain this anion. Since free ReO$_4^-$ gives only one band,[24] the appearance of the two bands is probably due to the lowering of symmetry of the ion due to weak coordination to the Pt$_3$ triangle. The ^{31}P NMR spectrum of **6** contained only a singlet, consistent with the presence of C_3 symmetry in the structure. The ^{1}H and ^{31}P NMR spectra of **6**[PF$_6$] and **6**[ReO$_4$] in CD$_2$Cl$_2$ solution were identical, indicating that the ReO$_4^-$ ion probably dissociates in solution.

(23) (a) Herrmann, W. A.; Roesky, P. W.; Kühn, F. E.; Scherer, W.; Kleine, M. *Angew. Chem., Int. Ed. Engl.* **1993**, *32*, 1714. (b) Wieghardt, K.; Pomp, C.; Nuber, B.; Weiss, J. *Inorg. Chem.* **1986**, *25*, 1659.

(24) K. Nakamoto, *Infrared and Raman Spectra of Inorganic and Coordination Compounds*, 4th ed.; Wiley: New York, 1986.

Table 2. Binding Energies (eV)^a and ν(CO) Stretching Frequencies of Selected Samples

compd	Re 4f$_{7/2}$	Pt 4f$_{7/2}$	ν(CO)/cm^{-1}
Re (metal)	39.7^b		
ReO$_2$	42.5^b		
ReO$_3$	44.9^b		
NH$_4$ReO$_4$	46.6		
Pt (metal)		70.9^c	
PtCl$_2$(dppm)		73.4^d	
[Pt$_3$(CO)(μ-dppm)$_3$]$^{2+}$		72.9^d	1765
[Pt$_3$\{Re(CO)$_3$\}(μ-dppm)$_3$]$^+$	41.6	72.6	1979, 1873, 1867
[Pt$_3$\{Re(CO)$_3$\}(μ-O)(μ-dppm)$_3$]$^+$	41.6	72.6	1978, 1864
[Pt$_3$\{Re(CO)$_3$\}(μ-O)$_2$(μ-dppm)$_3$]$^+$	41.6	73.0	1974, 1862, 1852
[Pt$_3$\{Re(CO)$_3$\}(μ-O)$_3$(μ-dppm)$_3$]$^+$	41.7	73.0	1987, 1856
[Pt$_3$\{ReO$_3$\}(μ-O)(μ-dppm)$_3$]$^+$	45.6	73.3	
[Pt$_3$(ReO$_3$)(μ-dppm)$_3$]$^+$	44.6	73.0	

^{a} Corrected with respect to C 1s BE of 284.9 eV. The anion is PF$_6^-$. Unless indicated, the data are from this work. ^{b} Reference 5e. ^{c} Reference 5c. ^{d} Reference 25.

Chart 1
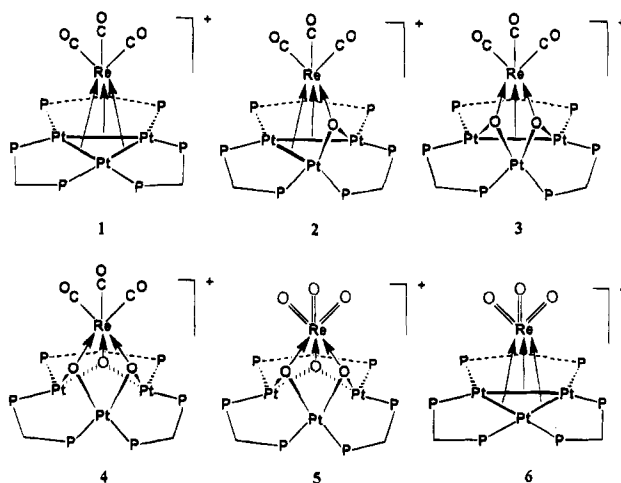
In the ^{31}P NMR spectrum, the value of ^1J(PtP) = 3134 Hz was higher and ^3J(PPtPtP) = 133 Hz was lower than in **1** (values of 2411 and 198 Hz respectively), indicative of somewhat weaker but still significant PtPt bonding. Since both CO and terminal oxo are two-electron ligands, both **1** and **6** are 54-electron clusters and so similar metal—metal bonding is expected.

XPS Studies of the Cluster Cations. The series of cluster cations **1**−**6** offers an unusual opportunity to study the core binding energies in the platinum and rhenium atoms as a function of the degree of oxidation as measured by the X-ray photoelectron spectra. The results are given in Table 2 which, for comparison purposes, also includes binding energies for some rhenium oxides.[5]

The Re 4f$_{7/2}$ binding energies in **1**−**4** are essentially unchanged as more oxygen atoms are added. At first glance, this is surprising since oxidation should lead to an increase in binding energy. However, in terms of the valence bond interpretation of bonding shown in Chart 1, the formal oxidation state of rhenium remains at +1 in this series and the constancy of the binding energies can be rationalized on that basis. Remember that the values of ν(CO) for the Re(CO)$_3$ groups also change only to a small extent in the series **1**−**4** as summarized in Table 2 and so both parameters indicate little real change in the electron density at rhenium. The Pt 4f$_{7/2}$ binding energy increases from 72.6 eV in **1** to 73.0 eV in **4** as the formal oxidation state of platinum increases from 0 to +2. The binding energy in **4** is still lower than in the authentic platinum(II) complex [PtCl$_2$(dppm)], which has a binding energy of 73.4 eV. In complexes **2** and **3**, two types of platinum atoms are

expected but only an average binding energy was obtained. The binding energies for the clusters overlap the ranges for Pt(I) and P(II) complexes.[25]

In contrast to the above results, there was a large change in the Re $4f_{7/2}$ binding energy from 41.6 eV in **1** to 45.6 eV in the hexaoxo cluster **5** and to 44.6 eV in the terminal oxo cluster **6**. For comparison, the binding energy in NH_4ReO_4 and ReO_3 is 46.6 and 44.9 eV,[5e] respectively. It is very clear that rhenium is in a high oxidation state in both **5** and **6**. The Pt $4f_{7/2}$ binding energy increases from 72.6 eV in **1** to 73.0 eV in **6**. Although this change is less dramatic, given the overlapping ranges of binding energies for different formal oxidation states in platinum complexes,[25] it is clear that the ReO_3 group in **6** is considerably more electron-withdrawing than the $Re(CO)_3$ group in **1**. The Pt $4f_{7/2}$ binding energies in the trioxo clusters **4** and **6** are indistinguishable. The Pt $4f_{7/2}$ binding energy is 73.3 eV in **5**, so the oxidation state of Pt approaches Pt(II), showing that the ReO_3 group in **5** is also more electron-withdrawing than the $Re(CO)_3$ group in **4**. The oxidation states of the metals in **5** and **6** may be formally described as $Pt^0{}_3Re^{VII}$ and $Pt^{II}{}_3Re^{VII}$, respectively. Hence, the formation of **5** and **6** is accompanied by an increase in the sum of the metal oxidation states in **1** by 6 units in forming **6**, and by 12 units in forming **5**! To our knowledge, this appears to be the first example of oxidation of a cluster complex to such an extent without cluster fragmentation.

The insensitivity of the binding energy to the the oxygen content in clusters **1–4** also brings up an interesting point regarding the use of temperature-programmed reduction (TPR) and XPS in the study of metal catalysts supported on oxide surfaces.[5a,b,d] The TPR, which gives a quantitative determination of the extent of reduction of metal oxides through measuring H_2 consumption, is often utilized in conjunction with XPS to determine the oxidation states of metals in supported catalysts. For clusters with varying oxygen content, corresponding H_2 consumptions are expected to vary. However, this might not be the case for the metal binding energy, as indicated by this study. Therefore, caution should be exercised in explaining results from the joint use of TPR and XPS.

Bonding in the Cluster Cations. The cluster complex **1** has only 54 valence electrons and so is clearly coordinatively unsaturated. The oxidation to **2, 3**, and **4** involving sequential addition of 4-electron μ_3-oxo ligands leads to clusters with 58-, 62-, and 66-electron counts, respectively, since no ligands are lost in this process. Previously, the effect of a 12-electron increase in cluster electron count could only be studied by using structurally similar clusters of different metals. A well-known example is found in the clusters $[Cp_4Fe_4(CO)_4]$ (60-electron, 6 M–M bonds) vs $[Cp_4Co_4S_4]$ (72 electrons, 0 M–M bonds).[26] Clusters **1** (54 electrons) and **4** and **5** (66 electrons) provide a particularly good example because all are based on the Pt_3Re core and because the intermediate 58- and 62-electron clusters **2** and **3** are also known.

The bonding in **1** can be considered in terms of donation of charge from the three Pt–Pt bonds of a $Pt_3(\mu$-dppm$)_3$ fragment to the three empty acceptor orbitals of an $Re(CO)_3{}^+$ fragment as shown in Chart 1. In this way, each platinum shares 16 electrons and the rhenium shares 18 electrons. If an oxygen atom is inserted into a Pt–Pt bond to give a Pt–O–Pt unit, the oxygen atom may then donate 2 electrons to $Re(CO)_3{}^+$; the result is that addition of each μ_3-O ligand causes cleavage of a Pt–Pt bond and also a Pt–Re bond but leaves the platinum

and rhenium with a share of 16 and 18 electrons, respectively, throughout. The progressive weakening of metal–metal bonding predicted by this interpretation is shown in Chart 1 and is supported by the structural and spectroscopic data discussed earlier. The formal oxidation state of rhenium remains at +1 throughout this oxidation but the average oxidation state of the platinum atoms increases, such that it is considered $[Pt_3]^0$, $[Pt_3]^{2+}$, $[Pt_3]^{4+}$, and $[Pt_3]^{6+}$ in **1, 2, 3**, and **4** respectively. Thus, in the trioxo cluster **4** all the platinum atoms may be considered as Pt(II) with each having 16 electrons and distorted square-planar geometry, and the $Re(I)(CO)_3$ center completes an inert gas configuration by accepting a pair of electrons from each of the three oxo ligands. Similar bonding schemes have been proposed for the dioxo-capped cluster $[Pt_4Cl_2(\mu_3$-O)_2(dmso)_6]^{20a}$ and the complex $[(\eta$-C_5H_5)WOs_3(CO)_6(\mu_2$-O)(\mu_3$-CCH_2Tol)]$ (Tol = p-C_6H_4$-CH_3).[27] The hexaoxo cluster **5** has the same valence electrons as the trioxo cluster **4**, and its bonding can be described similarly except that a cationic $Re^{VII}O_3$ center acts as the electron acceptor (Chart 1). The intense red-black color of cluster **1** is associated with the metal–metal bonds and as these bonds are cleaved during the oxidation the colors become much paler until **5**, which is white in color. In the (hypothetical) transformation of **4** to **6** the cluster electron count decreases from 66 back to 54 electrons (a terminal oxo ligand donates only two electrons and three carbonyls are lost). In terms of the bonding scheme discussed above, **6** can be considered in terms of donation of three electron pairs from the Pt–Pt bonds of a $Pt_3(\mu$-dppm$)_3$ fragment to the three acceptor orbitals of a $ReO_3{}^+$ fragment; the bonding is therefore similar to that in **1** except that the formal oxidation state of rhenium is +7 instead of +1. The regeneration of metal–metal bonds in **6** is reflected in its intense color.

In order to gain a better understanding of the bonding in the novel oxo cluster **6**, molecular orbital analyses of the cluster cations **1** and **6**, along with the corresponding rhenium fragments, have been carried out.[28] The results are illustrated in Figures 3 and 4. Both the $Re(CO)_3{}^+$ and the $ReO_3{}^+$ fragments are of C_{3v} symmetry, and correlation diagrams for their formation from Re^+ with three CO and three O ligands respectively are shown in Figure 3. The case of $Re(CO)_3{}^+$ is well-known.[28b] The 5d level of Re splits to the t_{2g}-like set $(1a_1 + 1e)$ and $e_g{}^*$-like set $(2e)$ while the orbital $2a_1$ has mostly rhenium 6s, $6p_z$ character. The levels $1a_1$, $1e$, and $2a_1$ are stabilized by interactions with the empty carbonyl π^* orbitals. The $1a_1$ and $1e$ levels are occupied (Re^+ has the d^6 configuration) and the three potential acceptor orbitals are $2e$ and $2a_1$. The situation in $ReO_3{}^+$ is different in several respects. The 5d level of Re again splits to the t_{2g}-like set $(1a_1 + 1e)$ and $e_g{}^*$-like set $(2e)$ and again the orbital $2a_1$ has mostly rhenium 6s, $6p_z$ character. However, the levels $1a_1$, $1e$, and $2a_1$ are now destabilized by interactions with the filled oxygen $2p_\pi$ orbitals and the orbitals $1a_1$, $1e$, $2e$, and $2a_1$ are all vacant and available to act as acceptor orbitals.

The frontier orbitals for the $Pt_3(\mu$-H_2PCH_2PH_2)_3$ (abbreviated to Pt_3 in the following discussion) used as a model for $Pt_3(\mu$-dppm$)_3$, which has D_{3h} symmetry, are shown in Figure 4. The Pt–Pt bonding MO's are the $e' + a_1'$ orbitals but the Pt–Pt antibonding MO a_2' is calculated to lie slightly below a_1' in the hypothetical fragment and is the HOMO. In **1**, the overlap of

(25) Jennings, M. C.; Schoettel, G.; Roy, S.; Puddephatt, R. J. *Organometallics* **1991**, *10*, 580.

(26) Vahrenkamp, H. *Adv. Organomet. Chem.* **1983**, *22*, 169 and references therein.
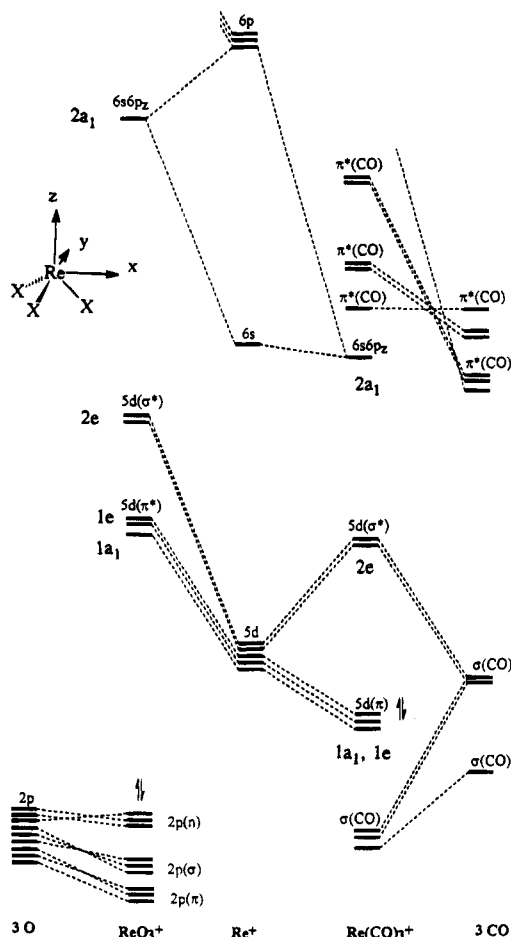
(27) Shapley, J. R.; Park, J. T.; Churchill, M. R.; Ziller, J. W.; Beanan, L. R. *J. Am. Chem. Soc.* **1984**, *106*, 1144.

(28) EHMO calculations were based on the model cluster $[Pt_3(ReL_3)(\mu$-H_2PCH_2PH_2)_3]^+$ (L = CO, O). For previous theoretical work on Pt_3L_6 clusters and on $M(CO)_3$ fragments, see: (a) Evans, D. G. *J. Organomet. Chem.* **1988**, *352*, 397. (b) Albright, T. A.; Burdett, J. K.; Whangbo, M.-H. *Orbital Interactions in Chemistry*; Wiley: New York, 1985; Chapter 20.

Models for Oxide Interactions in Bimetallic Catalysts

J. Am. Chem. Soc., Vol. 117, No. 23, 1995 6323

Figure 3. A correlation diagram for [ReO₃]⁺ and [Re(CO)₃]⁺.

Figure 4. A correlation diagram for [Pt₃(ReL₃)(μ-H₂PCH₂PH₂)₃]⁺ (L = O, CO).

the Pt₃ e′ and a₁′ orbitals with the 2e and 2a₁ orbitals, respectively, of Re(CO)₃⁺ leads to bonding and antibonding combinations. The bonding levels are filled, the HOMO being of a₁ symmetry as shown in Figure 4. Of course, this is consistent with the simple bonding picture outlined in Chart 1, except that the Pt₃ donor orbital a₁′ is actually calculated to be vacant in Pt₃(μ-H₂PCH₂PH₂)₃. The situation is similar in the Pt₃(ReO₃)⁺ case (Figure 4) except that the primary acceptor orbitals are now 1a₁ and 1e of ReO₃⁺. However, considerable orbital mixing occurs, such that the HOMO in Pt₃(ReO₃)⁺ of a₁ character has much Re 6s, 6p_z character as well as 5d_{z^2} character. Despite the major difference in the rhenium acceptor orbitals in the two cases, the pattern of metal—metal bonding is clearly similar. Thus, in each case, the three highest occupied MO's are Pt₃Re bonding orbitals of e + a₁ symmetry and the LUMO is a Pt₃Re antibonding orbital of e symmetry. Because the 1a₁ level of ReO₃⁺ is considerably lower in energy than the 2a₁ level of Re(CO)₃⁺, ReO₃⁺ is the stronger acceptor. *Ab initio* calculations on CpRe(CO)₃ and CpReO₃ have led to the same conclusion.[29] It should be noted that this polarization leads to a stabilization of the vacant a₂″ orbital (a combination of 6p_z orbitals) of the Pt₃ fragment. These vacant 6p_z orbitals on each of the platinum atoms are the source of coordinative unsaturation on platinum and are available for further ligand addition reactions.[28a] In contrast the a₂″ level is destabilized in Pt₃Re-(CO)₃⁺ and so the Pt₃ fragment should be deactivated toward ligand addition in this case.

There is an analogy between the donor orbitals of the D₃ₕ symmetry Pt₃(μ-H₂PCH₂PH₂)₃ fragment (a₁′ + e′) and the D₅ₕ

symmetry C₅H₅⁻ ligand (a₂″ + e₁″) and both have the correct symmetry to overlap with the acceptor orbitals of the C₃ᵥ symmetry ReO₃⁺ or Re(CO)₃⁺ fragments. This isolobal analogy may be useful in predicting new clusters based on capping by ReO₃⁺ and related units. In order to develop this analogy, calculations on CpReO₃ have been carried out and the correlation diagrams for interaction of ReO₃⁺ with both the Pt₃(μ-H₂-PCH₂PH₂)₃ fragment and the C₅H₅⁻ ligand are shown in Figure 5. It is immediately obvious that there are significant energy differences between the donor orbitals of Pt₃(μ-H₂PCH₂PH₂)₃ and C₅H₅⁻. In particular, the a₂″ level of Cp⁻ lies below the e₁″ level while the a₁′ level of Pt₃ lies well above the e′ level. This leads to some differences in the detailed picture but the analogy is still valid. It is noted that in both CpReO₃ and Pt₃-(ReO₃)⁺ there is greater d-character in the three highest occupied MO's (a + e) than in the Re(CO)₃ analogs due to the role of the 1a₁ + 1e orbitals of ReO₃⁺ as acceptors. This leads to somewhat longer bonds to the ReO₃⁺ unit in both cases. Thus the mean Re—C(Cp) distances are 2.41 and 2.28 Å in CpReO₃ and CpRe(CO)₃ and the mean Re—Pt distances are 2.726 and 2.673 Å in [Pt₃(μ-dppm)₃(ReO₃)]⁺ and [Pt₃(μ-dppm)₃{Re-(CO)₃}]⁺, respectively.[30] Calculations were also carried out on the model complexes [Pt₃(μ-H₂PCH₂PH₂)₃(μ_3-O)₃(ReX₃)]⁺ (X = CO or O). The degree of charge transfer from the fragment [Pt₃(μ-H₂PCH₂PH₂)₃(μ_3-O)₃] (calculated to be a stable molecule although not yet known) to [ReX₃]⁺ was almost identical to the case with [Pt₃(μ-H₂PCH₂PH₂)₃] but significantly less than that from Cp⁻. This is consistent with the experimental evidence based on IR and XPS data. For example, the ν(Re=O) frequencies (in cm⁻¹) in [LReO₃]⁺ are 909, 878 for L =

(29) (a) Wiest, R.; Leininger, T.; Jeung, G.-H.; Bénard, M. *J. Phys. Chem.* **1992**, *96*, 10800. (b) Szyperski, T.; Schwertfeger, P. *Angew. Chem., Int. Ed. Engl.* **1989**, *28*, 1228.

(30) (a) Fitzpatrick, P. J.; Le Page, Y.; Butler, I. S. *Acta Crystallogr., Sect. B* **1981**, *B37*, 1052. (b) Kuhn, F. E.; Herrmann, W. A.; Hahn, R.; Elison, M.; Blumel, J.; Herdtweck, E. *Organometallics* **1994**, *13*, 1601.
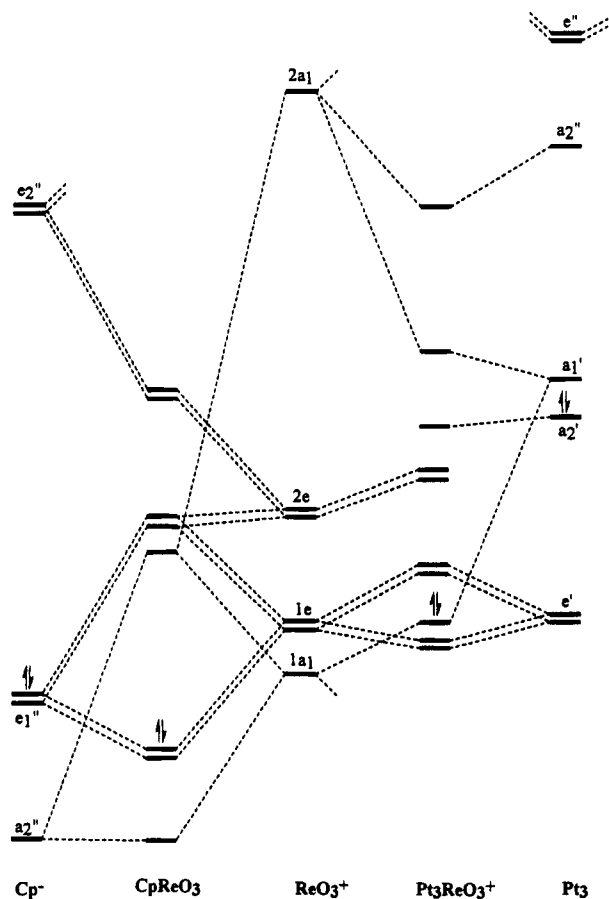
Figure 5. An orbital interaction diagram for CpReO₃ and [Pt₃(ReO₃)(μ-H₂PCH₂PH₂)₃]⁺.

C₅Me₅⁻, 935, 890 for L = [Pt₃(μ-dppm)₃], 937, 900 for L = [Pt₃(μ-dppm)₃(μ-O)₃], and 955, 930 for L = (C₂H₄NH)₃. Thus the platinum clusters appear to be intermediate in donor ability between Cp⁻, Cp*⁻ and simple ligands such as (C₂H₄NH)₃.[23]

Discussion

This work has shown how a remarkable series of oxo clusters can be built up by progressive oxidation of the Pt₃Re cluster **1**. There are a few other known reactions involving O₂ which yield oxo clusters.[6i,j,7a] A typical example is seen in the reaction of [Ru₃(CO)₈(μ-dppm)₂] with O₂ to give [Ru₃(CO)₆(μ₃-O)(μ-dppm)₂], in which a μ₃-oxo ligand replaces two carbonyl ligands with no net change in cluster electron count.[6j] None of the known reactions generates dioxo or trioxo clusters. On the other hand, chemisorption of O₂ on metal surfaces causes the cleavage of the O—O bond to give dioxo species, and it is these species that are active for many catalytic oxidations.[31] The conversion of **1** to **3** by O₂ gives the first model for dissociative chemisorption of O₂ on a metal surface. Together with the oxidation sequence of **1** to **2** to **3** to **6** and then [ReO₄]⁻ (Scheme 1 and eq 2), which demonstrates how a low oxidation state rhenium atom can be oxidized to perrhenate in a stepwise manner while bound to a Pt₃ cluster, the clear identification of these oxo clusters may provide significant insight into oxide-supported bimetallic catalysts. It is well-known that metals such as Pt and Pd catalyze the reduction of metal oxides on oxide surfaces.[5] An example is the platinum-catalyzed reduction of rhenium oxides in the formation of the important reforming

catalyst Pt—Re/Al₂O₃. It has been suggested that rhenium oxides such as [ReO₄]⁻ migrate over the support surface and are reduced in contact with a platinum particle, whereupon bimetallic Pt—Re clusters are formed.[5c,d] A similar example is found in the Pd-catalyzed reduction of iron oxide, where iron is completely reduced to Fe(0) only when its oxide is in direct contact with Pd(0) centers.[31] This reduction process could be the reverse of the oxidation sequence observed for **1**. It is also conceivable that various oxides may exist in contact with the Pt or Pd clusters during reduction. This study shows that a ReO₃ fragment can be metal—metal bonded to a Pt cluster or bonded through the oxygen atoms. The interconversion between such functional groups may well be involved in catalytic reduction of metal oxides. Further, given the easy formation of oxo complexes from **1** and the fact that heterogeneous catalysts often undergo reversible oxidation and reduction, metal clusters containing oxygen atoms on oxide surfaces might be a general phenomenon.

Experimental Section

The compounds [Pt₃{Re(CO)₃}(μ-dppm)₃][PF₆] (**1**), [Pt₃(μ₃-H)(μ-dppm)₃][PF₆], and [MeReO₃] were prepared by the previously reported procedures.[8,15,16] IR spectra were recorded by using a Perkin-Elmer 2000 spectrometer, and the NMR spectra were recorded, unless otherwise indicated, in CD₂Cl₂ solution at ambient temperature by using a Varian Gemini-300 spectrometer; chemical shifts are referenced to TMS (¹H) and 85% H₃PO₄ (³¹P{¹H}). Elemental analyses were performed by Galbraith Laboratories.

[Pt₃{Re(CO)₃}(μ-O)₂(μ-dppm)₃][PF₆] · OEt₂ (3[PF₆]). Method A. A solution of **1** (30 mg) in CH₂Cl₂ (10 mL) was stirred in the air for 1 week. The solution turned slowly from red brown to orange. Complex 3[PF₆] was produced in crystalline form upon concentration of the solution followed by adding diethyl ether. Yield: 70%. The reaction was faster when the reaction was carried out under an atmosphere of pure O₂; no reaction occurred when an atmosphere of N₂ was maintained. The experiment was conducted in a similar manner except that a flow of O₂ was introduced to the CH₂Cl₂ solution of **1**. Yield: 70%. IR (Nujol): ν(CO)/cm⁻¹ 1974 s, 1862 s, 1852 s. NMR (acetone-d₆): δ(¹H) 6.40 [br, 1H, H₂CP₂]; 4.62 [m, 1H, H₂CP₂]; 3.32 [br, 2H, H₂CP₂]; 3.10 [br, 2H, H₂CP₂]. NMR (CD₂Cl₂): δ(³¹P) 5.3 [m, ¹J(PtP) = 2733 Hz, ²J(PtP) = 824 Hz, ³J(PP) = 176 Hz, Pᵇ], 4.8 [s, ¹J(PtP) = 3440 Hz, Pᶜ], 1.8 {s, ¹J(PtP) = 3887 Hz, ²J(PP) = 45 Hz, Pᵃ]. (See text for the NMR labeling.) Anal. Calcd for C₈₂H₇₆-F₆O₆P₇Pt₃Re: C, 43.6; H, 3.4. Found: C, 43.3; H, 3.2.

Method B. To a solution of **1** (30 mg) in CH₂Cl₂ (10 mL) was added Me₃NO (4 mg). The solution immediately became lighter in color. The mixture was stirred for 6 h. The solution was then concentrated, and the product was precipitated by adding diethyl ether and was washed with MeOH. Orange crystals of 3[PF₆] were obtained from CH₂Cl₂/diethyl ether. Yield: 85%. Complex **3** is stable for at least a few weeks in air or in the presence of Me₃NO.

Method C. The reaction was conducted in a similar manner to Method B except that excess PhIO was used instead of Me₃NO, and the mixture was stirred for 30 min. Complex 3[PF₆] was isolated in 85% yield. When 1 equiv of PhIO was used, some **1** was unreacted and the major product was **3**, as determined by NMR analysis. Prolonged reaction of **1** with PhIO led to decomposition of the product **3**.

Method D. The reaction was conducted in a similar manner to Method B except that excess KOH was used instead of Me₃NO, and the mixture was stirred overnight. Complex 3[PF₆] was isolated in 75% yield. Bis(triphenylphosphine)iminium chloride also catalyzed the oxidation of **1**. However, the formation of 3[PF₆] was often accompanied by the decomposition of **1**, yielding the previously characterized complex [Pt₃(μ₃-Cl)(μ₃-CO)(μ-dppm)₃]⁺.[32]

It is noted that crystalline 3[PF₆] could be readily obtained from CH₂Cl₂/diethyl ether and methods B—D provide easy routes to pure 3[PF₆].

(31) (a) Boreskov, G. K. In *Catalysis, Science and Technology*; Anderson, J. A., Boudart, M., Eds.; Springer-Verlag: New York, 1982. (b) Garten, R. L.; Ollis, D. F. *J. Catal.* **1974**, *35*, 232.

(32) Manojlović-Muir, Lj.; Muir, K. W.; Lloyd, B. R.; Puddephatt, R. J. *J. Chem. Soc., Chem. Commun.* **1985**, 536.

[Pt₃{Re(CO)₃}(μ₃-O)(μ-dppm)₃][PF₆] (2[PF₆]). To a solution of **1** (50 mg) in CH₂Cl₂ (15 mL) was added 1 equiv of Me₃NO. The solution was stirred for 2 h. ³¹P NMR monitoring showed that the reaction was completed, with complexes **2[PF₆]** and **3[PF₆]** being formed in a ratio of about 5:1. When exposed to O₂, complex **2[PF₆]** was converted to **3[PF₆]** in about 24 h. IR (Nujol): $\nu(CO)/cm^{-1}$ 1978 s, 1864 s, br; NMR (acetone-d_6): $\delta(^1H)$ 4.85 [br, 2H, **H₂CP₂**]; 4.41 [br, 1H, **H₂CP₂**]; 4.25 [br, 2H, **H₂CP₂**]; 3.80 [br, 1H, **H₂CP₂**]. NMR (acetone-d_6): $\delta(^{31}P)$ 14.7 [m, $^1J(PtP) = 2430$ Hz, $^3J(P^aP^c) = 187$ Hz, P^a], 12.2 [m, $^1J(PtP) = 2600$ Hz, $^3J(P^aP^c) = 187$ Hz, $^2J(P^bP^c) = 37$ Hz, P^c], 3.0 [m, $^1J(PtP) = 4172$ Hz, $^2J(P^bP^c) = 37$ Hz, P^b].

[Pt₃{Re(CO)₃}(μ₃-O)₃(μ-dppm)₃][PF₆] (4[PF₆]). To a solution of **1** (30 mg) in CH₂Cl₂ (15 mL) was added H₂O₂/H₂O (0.6 mL, 30% solution). An immediate color change to orange was observed. The mixture was stirred for 6 h. Distilled water was then added to remove the unreacted H₂O₂. The CH₂Cl₂ solution was separated from the H₂O layer and then concentrated, followed by adding diethyl ether to precipitated **4[PF₆]** as a yellow powder. Yellow crystals of the complex were easily obtained from CH₂Cl₂/diethyl ether or acetone/hexane. Yield: 75%. NMR monitoring showed that complex to **3[PF₆]** appeared immediately on mixing **1** with H₂O₂, and complete conversion to **4[PF₆]** took about 1 h. IR (Nujol): $\nu(CO)/cm^{-1}$ 1987 s, 1856 s, br. NMR (CD₂Cl₂): $\delta(^1H)$ 3.30 [br, 3H, **H₂CP₂**]; 2.18 [br, 3H, **H₂CP₂**]. NMR (CD₂Cl₂): $\delta(^{31}P)$ 2.2 [s, $^1J(PtP) = 3401$ Hz]. Anal. Calcd for C₇₈H₆₆F₆O₆P₇Pt₃Re: C, 42.6; H, 3.0. Found: C, 42.9; H, 3.3.

Complex **4** can be prepared by the reaction of cluster **3** with H₂O₂. The procedure was similar to that described above. Complex **4** could be isolated in yields up to 95%. Complex **4** was also formed by UV irradiation of a THF solution of **1** in the air for about 18 h.

[Pt₃{ReO₃}(μ₃-O)₃(μ-dppm)₃][PF₆] (5[PF₆]). This complex was prepared in a manner similar to that for **4[PF₆]** where H₂O₂ was used except that the reaction time was longer, at about 16 h (yield 45%). Anal. Calcd for C₇₅H₆₆F₆O₆P₇Pt₃Re: C, 41.6; H, 3.1. Found: C, 41.8; H, 3.1. IR (Nujol): $\nu(Re=O$ of ReO₃)/cm^{-1} 937 m, 900 s. NMR (CD₂Cl₂): $\delta(^1H)$ 3.43 [br, 3H, **HCP₂**], 2.47 [br, 3H, **HCP₂**]. NMR (CD₂Cl₂): $\delta(^{31}P\{^1H\}) = 1.94$ [s, $^1J(PtP) = 3561$, dppm].

[Pt₃{ReO₃}(μ-dppm)₃][PF₆]·CH₂Cl₂ (6[PF₆]). Method A. Complex **1** (40 mg) was suspended in *o*-xylene (15 mL) and the mixture was heated under reflux for 10 h, during which time a deeper red brown solution was formed. The solution was cooled to room temperature and layered with pentane (20 mL). Complex **6[PF₆]** was precipitated as an orange solid, which could be recrystallized from CH₂Cl₂/diethyl ether. Yield: 90%, but not easy to reproduce. NMR monitoring showed that complex **3[PF₆]** was the first to be formed. IR (Nujol): $\nu(Re=O)(ReO_3)/cm^{-1}$ 925 s, 893 s; $\nu(Re=O)(ReO_4)/cm^{-1}$ 940 w, 890 s. NMR (CD₂Cl₂): $\delta(^1H)$ 6.11 [br, 3H, **H₂CP₂**]; 5.02 [br, 3H, **H₂CP₂**]. NMR (CD₂Cl₂): $\delta(^{31}P)$ −2.5 [s, $^1J(PtP) = 3134$ Hz, $^3J(PP) = 133$ Hz]. Anal. Calcd for C₇₆H₆₈F₆O₃Cl₂P₇Pt₃Re: C, 41.4; H, 3.1. Found: C, 41.6; H, 3.2.

Complex **6[ReO₄]** was prepared similarly except that **1** was refluxed for ca. 15 h. The complex might be crystallized from CH₂Cl₂/diethyl ether. Yield for **6[ReO₄]**: 30%. IR (Nujol): $\nu(Re=O)(ReO_3)/cm^{-1}$ 935 s, 893 s; $\nu(Re=O)(ReO_4^-)/cm^{-1}$ 915 s, 905 sh. The NMR spectra of **6[ReO₄]** were identical to those of **6[PF₆]**.

Method B. To a solution of [Pt₃(μ₃-H)(μ-dppm)₃][PF₆] (60 mg) in CH₂Cl₂ (15 mL) was added [MeReO₃] (12 mg). The mixture was stirred for 2 h. The solution was concentrated, followed by addition of diethyl ether to give an orange solid, which was further washed with diethyl ether. Yield: 80%. Well-shaped black crystals of **6[PF₆]** could be easily obtained from CH₂Cl₂/diethyl ether.

[Pt₃{Re(CO)₂P(OMe)₃}(μ₃-O)₂(μ-dppm)₃][PF₆] (7a[PF₆]). To a solution of **3[PF₆]** (35 mg) in CH₂Cl₂ (10 mL) was added P(OMe)₃ (0.1 mL). The mixture was stirred for 24 h. The solution was then concentrated, and the product was precipitated by adding diethyl ether and washed with diethyl ether. Red-orange crystals of **7a[PF₆]** were obtained from CH₂Cl₂/diethyl ether. Yield: 50%. IR (Nujol): $\nu(CO)/cm^{-1}$ 1894 s, 1805 s. NMR (CD₂Cl₂): $\delta(^1H)$ 6.45 [br, 1H, **H₂CP₂**]; 4.83 [br, 1H, **H₂CP₂**]; 3.29 [br, 2H, **H₂CP₂**]; 3.06 [br, 2H, **H₂CP₂**]; 3.48 [d, $^3J(PP) = 19$ Hz, P(OCH₃)₃]. NMR (CD₂Cl₂): $\delta(^{31}P)$ 135.3 [q, $^2J(PtP) = 82$ Hz, P(OMe)₃]; 3.7 [m, $^1J(PtP) = 2760$ Hz, $^2J(PtP) = 759$ Hz, $^3J(PP) = 194$ Hz, P^b]; 3.2 [s, $^1J(PtP) = 3411$ Hz, P^c]; 1.0 [s,

$^1J(PtP) = 3911$ Hz, $^2J(PP) = 34$ Hz, P^a]. Anal. Calcd for C₈₀H₇₅F₆-O₇P₈Pt₃Re: C, 42.1; H, 3.3. Found: C, 41.1; H, 3.5.

[Pt₃{Re(CO)₂P(OPh)₃}(μ₃-O)₂(μ-dppm)₃][PF₆] (7b[PF₆]). Compound **7b[PF₆]** was prepared in a manner similar to that for **7a[PF₆]**, except that P(OPh)₃ was used instead of P(OMe)₃. The compound was isolated as an orange powder. Yield: 60%. IR (Nujol): $\nu(CO)/cm^{-1}$ 1902 s, 1817 s. NMR (CD₂Cl₂): $\delta(^1H)$ 4.63 [m, 1H, **H₂CP₂**]; 4.42 [m, 1H, **H₂CP₂**]; 2.96 [br, 4H, **H₂CP₂**]. NMR (CD₂Cl₂): $\delta(^{31}P) = 105.9$ [q, $^2J(PtP) = 104$ Hz, P(OPh)₃]; 3.4 [m, $^1J(PtP) = 2754$ Hz, $^2J(PtP) = 855$ Hz, $^3J(PP) = 186$ Hz, P^b]; 2.8 [s, $^1J(PtP) = 3396$ Hz, P^c]; 0.73 [s, $^1J(PtP) = 3890$ Hz, $^2J(PP) = 30$ Hz, P^a].

[Pt₃{Re(¹³CO)₃}(μ₃-O)₂(μ-dppm)₃][PF₆]. The reaction of **3[PF₆]** with ¹³CO was conducted in an NMR tube. In a typical experiment, **3[PF₆]** (15 mg) was dissolved in CD₂Cl₂ (0.5 mL) in an NMR tube. ¹³CO was then added by syringe. The reaction took about 10 h to reach completion. NMR (CD₂Cl₂): $\delta(^{13}C, 22°C)$ 201.2 (s). NMR (CD₂Cl₂): $\delta(^{13}C, -90°C)$ 201.5 (s, 2C), 196.4 (s, 1C).

X-ray Crystal Structure Analysis of [Pt₃{Re(CO)₃}(μ-O)₂(μ-dppm)₃][PF₆]·OEt₂ (3[PF₆]·OEt₂). Orange, needle-like crystals of the complex **3[PF₆]**·OEt₂ were obtained from a CH₂Cl₂/diethyl ether solution. All X-ray measurements were made at 28 °C with mono-chromated Mo Kα radiation and an Enraf-Nonius CAD4 diffractometer. Experimental details are summarized in Table 3.

The unit cell constants were determined by the least-squares treatment of 25 reflections with Bragg angles in the range 20.9 < θ < 23.3°. Intensities for 24 355 reflections with *h* (−24) −24, *k* (−33) −0, *l* (−28) −0 were measured by continuous ω/2θ scans. The scan speeds were adjusted to give σ(I)/I < 0.03, subject to a time limit of 30 s. Three reflections, (7 −8 −6), (−6 −10 −4) and (2 −6 −10), were used to monitor stability of the crystal and diffractometer. Their mean intensity showed a linear decrease of up to 10.7% over the 172 h of data collection. Lorentz, polarization, and crystal decomposition corrections were applied to the intensities. Empirical absorption corrections were made by the method of Walker and at the end of the isotropic refinement.[33] The internal agreement factor, R_{int}, for merging 620 duplicate intensities was 0.072 before and 0.025 after correction for absorption. Of 23 735 unique reflections measured, 11 822 for which $I > 2\sigma(I)$ were used in the subsequent analysis.

The positions of the non-hydrogen atoms were obtained using Patterson and difference Fourier methods. Hydrogen atoms of the dppm ligands were included in the calculated positions with C−H = 0.96 Å. Their isotropic displacement parameters were fixed at *ca.* $1.2U_{eq}$ of the parent carbon atoms. No allowance was made for the scattering of the diethyl ether hydrogens. The structure was refined by full-matrix least-squares, minimizing the function $\Sigma w(|F_o| - |F_c|)^2$, where $w = \sigma(|F_o|)^{-2}$. The eleven C and H atoms of each phenyl ring were refined as an idealized rigid group with C−C = 1.38 Å. The methylene H

(33) Walker, N.; Stuart, D. *Acta Crystallogr., Sect. A: Found. Crystallogr.* **1983**, *A39*, 158.

atoms were allowed to ride on the C atoms to which they are bonded. Anisotropic displacement parameters were refined for all non-hydrogen atoms. These parameters (Table 4) are large for the hexafluorophosphate anion and diethyl ether molecule; they suggest disorder of the two residues, but the alternative sites of their atoms were not obvious in the maps of electron density. The GX program package[34] was used in all calculations. The scattering factors and anomalous dispersion corrections were taken form the International Tables for X-ray Crystallography.[35]

X-ray Photoelectron Spectroscopy (XPS) Analysis. The spectra were taken on either powder or crystalline samples pressed onto copper foils by using a SSL SSX-100 instrument fitted with a Mg Kα X-ray source (1253.6 eV). The carbon 1s binding energy of 284.9 eV was used to calibrate the spectra.

(34) Mallinson, P. R.; Muir, K. W. *J. Appl. Crystallogr.* **1985**, *18*, 51.
(35) *International Tables for X-ray Crystallography*; Kynoch Press: Birmingham, England, 1974; Vol. 4.

Supplementary Material Available: Tables of atomic coordinates, anisotropic displacement parameters, bond lengths, and angles and figures showing the numbering sequence for $[Pt_3Re(\mu_3\text{-}O)_2(CO)_3(\mu\text{-}Ph_2PCH_2PPh_2)_3]^+$ and the probability ellipsoids for $[PF_6]^-$ and diethyl ether (16 pages); listing of observed and calculated structure factors (38 pages). This material is contained in many libraries on microfiche, immediately follows this article in the microfilm version of the journal, can be ordered from the ACS, and can be downloaded from the Internet; see any current masthead page for ordering information and Internet access instructions.

JA950199T